

Article

Physiological Response of *Saccharomyces cerevisiae* to Silver Stress

Janelle R. Robinson ¹, Omoanghe S. Isikhuemhen ^{1,*} , Felicia N. Anike ¹ and Kiran Subedi ² 

¹ Department of Natural Resources and Environmental Design, North Carolina Agricultural and Technical State University, 1601 East Market Street, Greensboro, NC 27411, USA; jrrobin3@aggies.ncat.edu (J.R.R.); fnanike@ncat.edu (F.N.A.)

² Analytical Services Laboratory, College of Agriculture and Environmental Sciences, North Carolina Agricultural and Technical State University, 1601 East Market Street, Greensboro, NC 27411, USA; ksubedi@ncat.edu

* Correspondence: omon@ncat.edu

Abstract: Silver nanoparticle (AgNP) production and their use as antimicrobial agents is a current area of active research. Biosynthesis is the most sustainable production method, and fungi have become candidates of interest in AgNP production. However, investigations into the physiological responses of fungi due to silver exposure are scanty. This present work utilized two strains of *Saccharomyces cerevisiae* (one used in commercial fermentation and a naturally occurring strain) to determine the physiological consequences of their transient exposure to AgNO₃. The assessments were based on studies involving growth curves, minimal inhibitory concentration assays, scanning electron microscopy (SEM) and transmission electron microscopy (TEM) imaging, and inductively coupled plasma optical emission spectroscopy (ICP-OES). Results indicated (a) the capability of *S. cerevisiae* to produce silver nanoparticles, even at elevated levels of exposure; (b) strain origin had no significant impact on *S. cerevisiae* physiological response to AgNO₃; and (c) coexposure to copper and silver significantly increased intracellular copper, silver, and calcium in treated yeast cells. In addition, electron microscopy and ICP-OES results revealed that both strains internalized silver after exposure, resulting in the shrunken and distorted physical appearance visible on SEM micrographs of treated cells. Though a promising candidate for AgNPs biosynthesis, this study analyzed the effects of transient silver exposure on *S. cerevisiae* growth physiology and morphology.

Keywords: *Saccharomyces cerevisiae*; silver nitrate; silver nanoparticle; physiological response; mycosynthesis



Citation: Robinson, J.R.; Isikhuemhen, O.S.; Anike, F.N.; Subedi, K. Physiological Response of *Saccharomyces cerevisiae* to Silver Stress. *J. Fungi* **2022**, *8*, 539. <https://doi.org/10.3390/jof8050539>

Academic Editor: Aaron Neiman

Received: 3 May 2022

Accepted: 21 May 2022

Published: 22 May 2022

Publisher's Note: MDPI stays neutral with regard to jurisdictional claims in published maps and institutional affiliations.



Copyright: © 2022 by the authors. Licensee MDPI, Basel, Switzerland. This article is an open access article distributed under the terms and conditions of the Creative Commons Attribution (CC BY) license (<https://creativecommons.org/licenses/by/4.0/>).

1. Introduction

The incidence of fungal–silver interactions is greatly increasing due to the growing interest in the use of fungi for silver nanoparticle (AgNP) production [1–3]. It is predicted that AgNPs will have an increased compound annual growth rate of 15.7% between 2020 and 2027 [4]. With some fungi having a high metal-tolerance capacity and the active research on AgNP mycosynthesis, it is logical to expect that fungi will play a significant role in the predicted market increase [5,6]. Species such as *Fusarium oxysporum*, *Botryodiplodia theobromae*, *Penicillium oxalicum*, and *Saccharomyces cerevisiae* have been investigated for their ability to produce AgNPs, the resulting AgNP characteristics, and levels of toxicity [7–10]. In addition, mycosynthesized AgNPs have been studied for their use as antimicrobial agents against medically relevant microorganisms, as synergistic enhancers for antibiotics, and as a promising treatment option for cancer therapy [11–15]. These types of fungal–silver interactions benefit humans in multiple ways. However, there is a lack of knowledge about how metal ions affect the morphology and physiology of different fungi, even in the common yeast *S. cerevisiae*, which has vast industrial applications and economic importance. Thus far, research has shown some impacts of silver exposure, including

effects on homeostatic systems and some physiological responses [16–19]. Transcriptome analysis has demonstrated that exposure can downregulate genes involved in the synthesis of membrane components, and imaging studies have shown that exposure can alter cellular morphology, even reducing dimorphism in pathogenic *Candida* sp. [16,20–23]. Most studies also utilize well-annotated laboratory strains of *S. cerevisiae* and pathogenic *Candida* spp.; however, reports on the impacts on most other fungal strains are limited.

Additionally, there is little understanding about silver exposure and silver uptake, capacity in *S. cerevisiae*. A recent review on this topic revealed that while some mechanisms of homeostasis have been unveiled, there is no consensus on the exact mechanisms [24]. The present study used two different strains of *S. cerevisiae*, one implemented in commercial fermentation processes and the other naturally present in palm wine from Ebelle, Nigeria. They were used to explore the physiological impacts of transient silver exposure and if the origin of each strain impacted the response. With the knowledge that both AgNPs and AgNO₃ can induce toxicity via the release of silver ions, AgNO₃ was used in the experiments.

2. Materials and Methods

2.1. *Saccharomyces cerevisiae* Strains and Growth Conditions

Two *S. cerevisiae* strains were obtained for this work. The first strain, termed commercial strain, was SUPERSTART™ active dry yeast obtained from Lallemand Biofuels and Distilled Spirits, a yeast designed for commercial production of biofuels or spirits. The second strain, termed naïve strain, was isolated from Ebelle palm wine, a naturally fermented alcoholic beverage produced from the collection of sap from the African oil palm, *Elaeis guineensis* Jacq. in Ebelle, Nigeria. The palm wine is made by using a container made from *Lagenaria siceraria* (calabash fruit) to collect the sap drippings from the holes made at the base of the inflorescence of the oil palm (Arecaceae family). Yeast existing in the calabash from previous use and yeast from the environment ferment the juice from the oil palm inside the calabash. Therefore, the yeast from Ebelle palm wine had no prior exposure to metal compared to those used for commercial fermentation processes. For identification, yeast underwent Sanger sequencing via Eurofins Genomics with primers ITS1F (CTTGGT-CATTAGAGGAAGTAA) and ITS4 (TCCTCCGCTTATTGATATGC). The National Center for Biotechnology Information (NCBI) Basic Local Alignment Search Tool (BLAST) returned the identification of commercial and naïve yeast as *S. cerevisiae* and with accession numbers CP006391.1 and LC215451.1, respectively [25]. In all experiments, yeasts in liquid media (20 g/L dextrose, 5 g/L yeast extract) were grown at 30 °C, 150 RPM in 50 mL Erlenmeyer flasks (Pyrex, Corning, Corning, NY, USA) in a shaking incubator (Thermo Scientific MAXQ 4000, Waltham, MA, USA). The cultures on solid media (20 g/L dextrose, 5 g/L yeast extract, and 15 g/L agar) were grown in a stationary incubator (Fisher Scientific 146E, Waltham, MA, USA) at 30 °C in 100 mm × 15 mm Petri dishes.

2.2. Chemicals and Reagents

Silver nitrate (Alfa Aesar ACS 99.9%+) was made into 1000 mg/L stock solution of AgNO₃ and was used for all experiments that required AgNO₃. All yeast were cultured on media that contained 20 g/L dextrose, 5 g/L yeast extract, and 15 g/L agar (solid media). Silver, calcium, and copper standards (1000 ppm each) purchased from High-Purity standards (Charleston, SC, USA) were used for elemental analysis.

2.3. Minimal Inhibitory Concentration Assay

The minimal inhibitory concentration (MIC) is the lowest concentration of AgNO₃, which completely inhibits cell growth. Before the MIC assay, cells were grown overnight in liquid media (20 g/L dextrose, 5 g/L yeast extract). After overnight growth, commercial yeast ($n = 10$) and naïve yeast ($n = 10$) were used to inoculate 96-well plates, with the final yeast OD_{A600} at 0.1 and incubated with AgNO₃ at concentrations of 0, 10, 20, 22.5, 25, 27.5, and 30 mg/L. 0 mg/L AgNO₃ (no addition of AgNO₃) was the positive control. Negative

controls were all reported concentrations with no yeast cells. Plates were incubated at 30 °C and 150 RPM for 48 h. After incubation, cells were subjected to 10-fold serial dilutions, spread on solid media, and incubated at 30 °C for 48 h to obtain single colonies. The lowest AgNO₃ concentration that resulted in no visible colony formation was selected as the MIC. The next lowest concentration was selected as the sub-MIC. The sub-MIC was toxic enough to inhibit a significant amount of growth without completely preventing growth. AgNO₃ concentration at sub-MIC was used for subsequent experiments.

2.4. Phenotypic Screening: Selection of Naturally Sensitive Isolates

The sub-MIC was used to select naturally sensitive (NS) isolates from the commercial and naïve yeast (i.e., isolates unable to grow at the sub-MIC) via replica plating [26,27]. Commercial and naïve yeast were grown overnight in liquid media, serially diluted, and spread on solid, nonselective media (master plate) for single colonies. The master plate was replica-plated onto an apparatus that held sterile velvet squares (Figure 1). The velvet then had an impression of the master plate. The plate with silver-containing selective media was pressed on top of the velvet with the master-plate impression. The impression was then imprinted onto the selective media and incubated for 48 h at 30 °C. After 48 h, the isolates that grew on the master plate but not the selective media were selected as naturally sensitive isolates. Ten NS commercial isolates (NS C1–C10) and ten NS naïve isolates (NS N1–N10) were selected for further experiments. This selection ensured the isolates chosen did not contain any preexisting natural resistance to the sub-MIC. All 20 isolates were grown in liquid culture and stored at a 1:1 ratio in 30% glycerol (Arcos Organics 99.9 + %) at −80 °C.

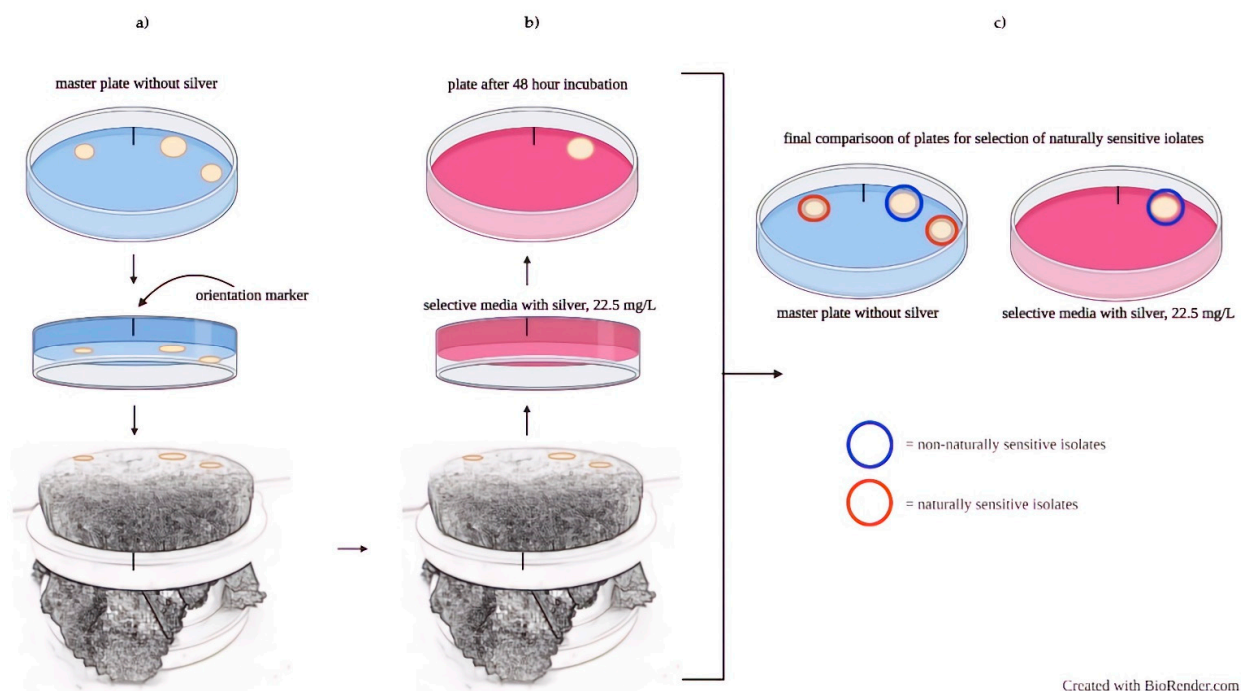


Figure 1. Replica plating for the selection of naturally sensitive isolates. (a) Single colonies from non-selective media impressed onto velvet. (b) Selective media containing silver received the impression from the velvet. (c) Incubation of selective media determined NS isolates on nonselective media.

2.5. Growth Curve Assay

Growth curve assays were conducted to determine the growth pattern of NS isolates with and without silver. In a 96-well plate (Costar 96-well Flat Bottom Assay Plate), 10 NS commercial yeast and 10 NS naïve yeast isolates were exposed to the sub-MIC and media without AgNO₃ and incubated inside a BioTek Synergy HY Plate Reader. The plate reader was set at 30 °C and used absorbance at 600 nm to collect a data point every hour for 72 h.

2.6. Scanning Electron Microscopy (SEM) and Transmission Electron Microscopy (TEM)

NS commercial yeast isolates (C1–C5) and NS naïve yeast isolates (N1–N5) were grown in 40 mL liquid media at the sub-MIC and in media without AgNO₃ for 48 h (Table 1). Samples were then delivered to the North Carolina State University Analytical Instrumentation Facility for SEM and TEM preparation and imaging. Sample preparation was based on several existing protocols [28–31]. All samples were pelleted and resuspended in 3% glutaraldehyde in a 0.1 M sodium cacodylate buffer. To prepare samples for SEM imaging, 100 µL of the suspended cells were mixed into 1 mL of 0.1 M sodium cacodylate buffer and filtered through a 0.4 µm nucleopore filter. The filtrate was discarded, and the filter was soaked in a container, on ice, with the same buffer for 15 min. The filter was moved twice to two new containers with the same buffer, each for another 15 min of incubation time. The filter was then dehydrated by washing samples with 30% and 50% ethanol (1 h each) and then placed into 70% ethanol at 4 °C for 2 h. The filter was then washed in cold 95% ethanol and cold 100% ethanol for 1 h each and washed twice at room temperature, in 100% ethanol. Samples on the filter then underwent critical-point drying in liquid CO₂. Each filter was then split and mounted on separate stubs and was left uncoated. For TEM imaging, samples in the 0.1 M sodium cacodylate buffer were pelleted, and the supernatant was removed. The samples were washed three times (15 min each) in the same buffer, pelleted, and the supernatant removed. Samples were then fixed in 0.1 M sodium cacodylate buffer with 2% osmium tetroxide for 4 h at 4 °C. Samples were then washed three more times as described above, pelleted, and had a 2% agarose solution added. Agarose was removed after 30 min, and samples underwent six 24 h washes in ethanol (50%, 70%, 95%, 100%, 100%, and 100%). Samples were then embedded in 50% Spurr's (epoxide resin with low viscosity) and washed in 100% ethanol for 24 h. This was repeated with 75% Spurr's, before samples were embedded in 100% Spurr's in BEEM capsules and incubated 70 °C overnight. Capsules were removed and samples sectioned with a Leica UC7 Cryo Ultramicrotome at 100 nm thickness. SEM imaging was completed on the FEI Verios 460 L field-emission scanning electron microscope (FESEM). TEM imaging was conducted on a Talos F200X G2.

Table 1. Parameters for microwave-assisted acid digestion.

Digestion Parameters	Values
Power	800 W
Temperature	180 °C
Ramp Time	20 min
Hold Time	15 min

2.7. Inductively Coupled Plasma Optical Emission Spectroscopy (ICP-OES)

ICP-OES was used to monitor the cellular influx of silver into yeast during silver exposure. Due to the potential use of copper transport channels by silver ions and the importance of calcium to cellular functioning, ICP-OES was also used to analyze the influx of copper (II) sulfate and calcium chloride [24]. NS commercial yeast isolates, C1–C5, and NS naïve yeast isolates, N1–N5, were grown overnight in liquid media and used to inoculate flasks that contained 22.5 mg/L AgNO₃, 22.5 mg/L CuSO₄, 22.5 mg/L CaCl₂, or 22.5 mg/L of both AgNO₃ and CuSO₄, with the final yeast OD₆₀₀ at 0.1.

Yeasts were incubated at 30 °C, 150 RPM for 48 h. After incubation, 20 mL of each sample was pelleted and underwent digestion. Predigestion was completed by incubating samples with nitric acid (68–70%) for 10 min; full digestion used a MARS 6 (CEM Microwave Technology Ltd., Matthews, North Carolina, USA) microwave digester with the parameters in Table 1. The clear, fully digested sample was diluted to a volume of 50 mL using double-deionized (DI) water and analyzed using Optima 8300 ICP-OES (Perkin Elmer, Inc., Shelton, CT, USA). Following digestion, samples underwent elemental ICP

analysis (Table 2) using the following emission lines for Ca, Cu, and Ag quantification: Ca (II) 317.933 nm, Cu (I) 324.372 nm, and Ag (I) 328.068 nm. The digestion and ICP analysis were completed in the Analytical Services Laboratory (ASL) at North Carolina Agricultural and Technical State University.

Table 2. Parameters for the elemental analysis by ICP.

ICP-OES Parameters	Values
RF Power	1500 Watts
Nebulizer Type	GemCone Low Flow
Nebulizer Gas Flow Rate	0.80 L/min
Plasma Gas Flow Rate	10 L/min
Auxillary Gas Flow Rate	0.25 L/min
Sample Flow Rate	1.60 mL/min

2.8. Statistical Analysis

Statistical analysis of the MIC assays and the growth curve used IBM SPSS Version 26. MIC analysis used a one-way analysis of variance (ANOVA) with a post hoc Tukey test. The growth curve analysis used a one-sample *t*-test to determine statistical significance between means. Graphs were generated with Microsoft Excel 2016.

3. Results

3.1. Minimal Inhibitory Concentration Assay

MIC assays were conducted to assess the sensitivity of *S. cerevisiae* to AgNO₃. Figure 2 represents colony growth of exposed cells as a percentage of the growth of cells that did not receive any AgNO₃ treatment. In both strains, no significant inhibition activity occurred at 0, 10, and 15 mg/L AgNO₃. Significant growth inhibition began at 17.5 mg/L AgNO₃. There was no observed growth at 25 and 30 mg/L AgNO₃, which indicated both yeast strains had a MIC of 25 mg/L AgNO₃ and a sub-MIC of 22.5 mg/L AgNO₃. At the sub-MIC, NS commercial and naïve yeast had comparable growth.

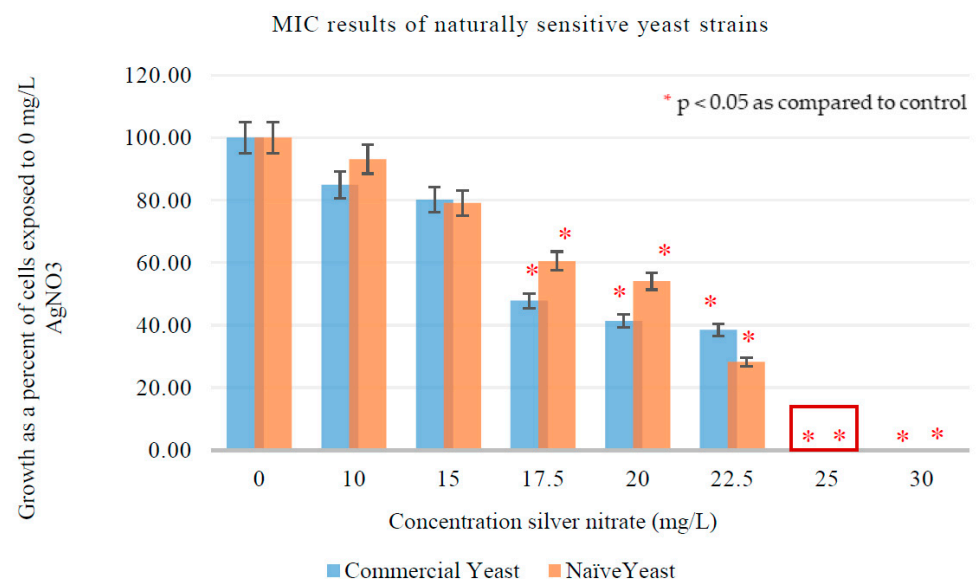


Figure 2. Minimal inhibitory concentration of AgNO₃ for NS commercial ($n = 10$) and naïve ($n = 10$) yeast. The red asterisk represents AgNO₃ concentrations that resulted in significantly less ($p < 0.05$) growth when compared to the control. The red box represents growth that occurred at the MIC. Error bars represent percentage error (5%).

3.2. Growth Curve Assay

After determining the sub-MIC, both yeast strains underwent growth curve assays to determine if silver exposure affected the normal growth pattern. Figure 3 shows the 72 h growth curve of NS commercial yeast ($n = 10$) and NS naïve yeast ($n = 10$) exposed to 0 mg/L AgNO₃ and the sub-MIC (22.5 mg/L). Yeast exposed to 0 mg/L AgNO₃ displayed typical growth over the 72 h [32]. Yeast exposed to the sub-MIC displayed significantly reduced growth ($p < 0.05$) compared to the controls. These results coincide with other data that show that excessive metal exposure decreases cell growth, resulting in growth curve abnormalities [33–35].

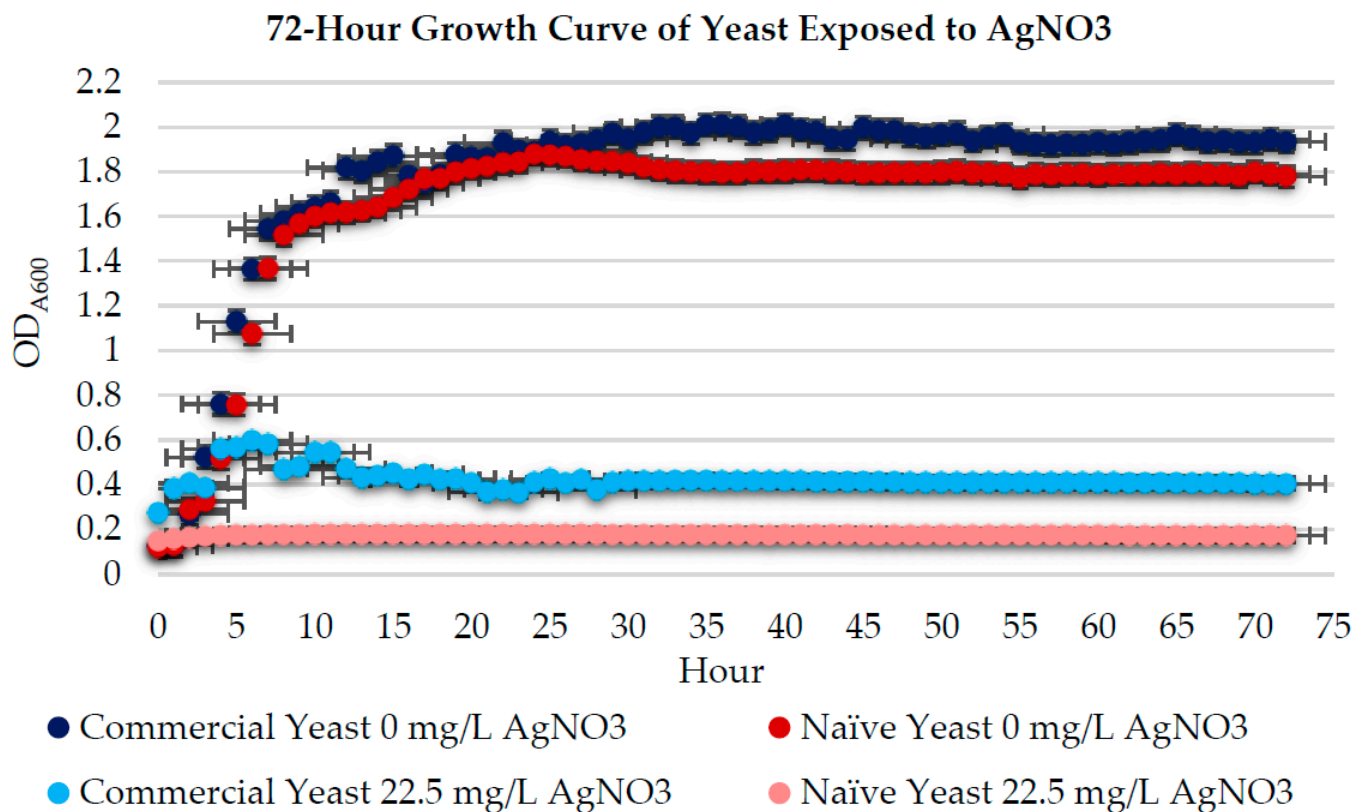


Figure 3. Growth curves for NS commercial ($n = 24$) and naïve ($n = 24$) yeast exposed to 0 mg/L AgNO₃ and the sub-MIC (22.5 mg/L AgNO₃). Error bars represent percentage error (5%).

NS commercial yeast had no significant growth after 11 h of exposure, and NS naïve yeast had no significant growth after 4 h of exposure. However, based on spectrophotometer results, NS commercial yeast had significantly more growth than NS naïve yeast after exposure to the sub-MIC.

3.3. Scanning Eletron Microscopy (SEM)

SEM studies indicated a distinction in size between commercial and naïve yeast (Figure 4a–d, respectively), where commercial yeast was larger in size. Results also indicated that both yeast strains exposed to 0 mg/L AgNO₃ (Figure 4a,c) had a smooth cell surface, typical morphology, for healthy *S. cerevisiae* cells [22,36]. However, exposure to the sub-MIC (Figure 5b,d) resulted in two distinct abnormal cell-surface morphologies:

1. A few cells had a smooth cell surface similar to unexposed yeast (Figure 5a,b).
2. A majority of cells had an abnormal physical appearance; cell surfaces of both yeast strains had drastic indentations or invaginations (Figure 5a,b).

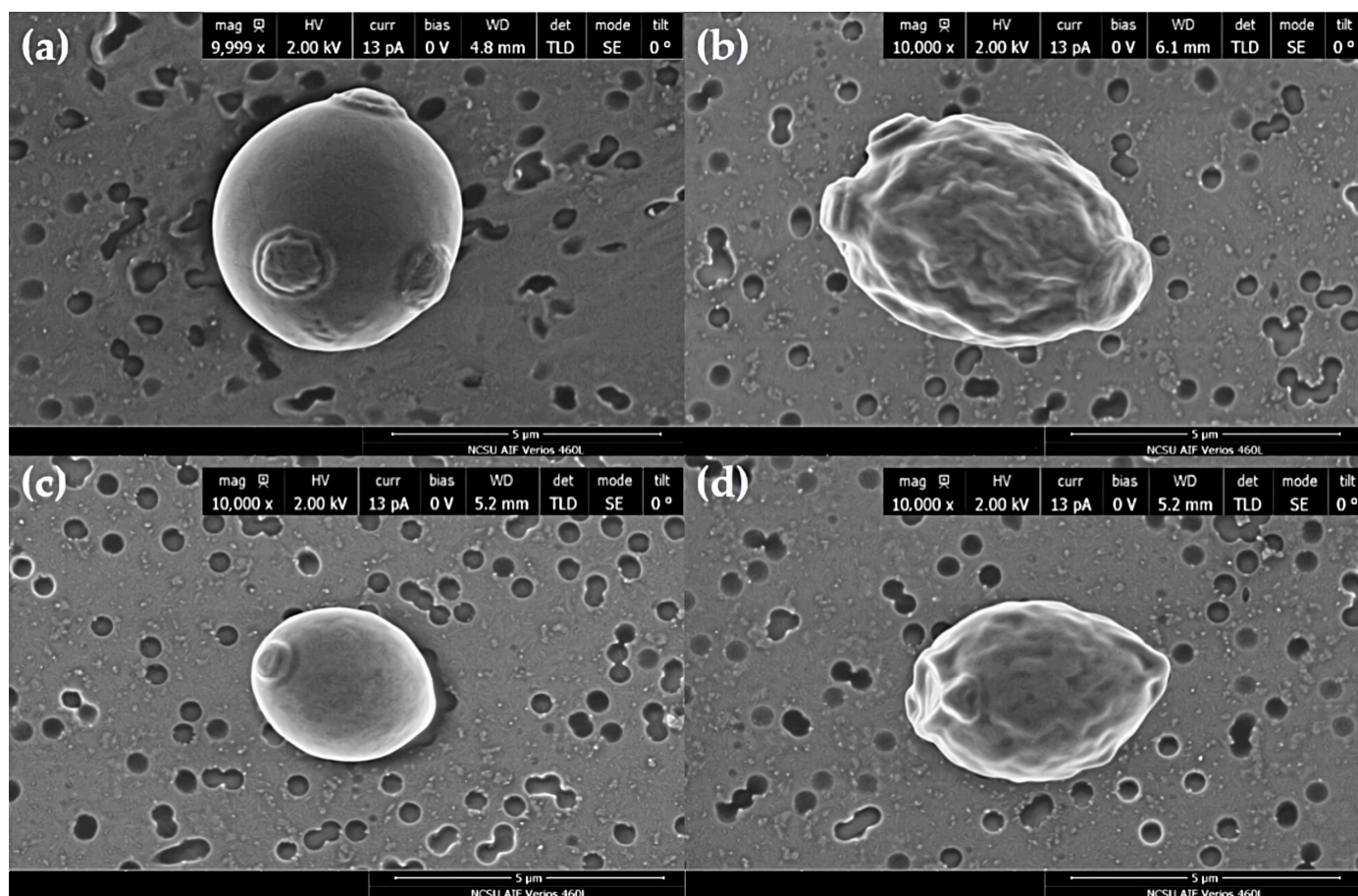


Figure 4. SEM micrographs of NS commercial and NS naïve yeast at 10,000× magnification. (a) and (c) are NS commercial and NS naïve yeast exposed to 0 mg/L AgNO_3 , respectively. (b,d) are NS commercial and NS naïve yeast exposed to 22.5 mg/L AgNO_3 , respectively.

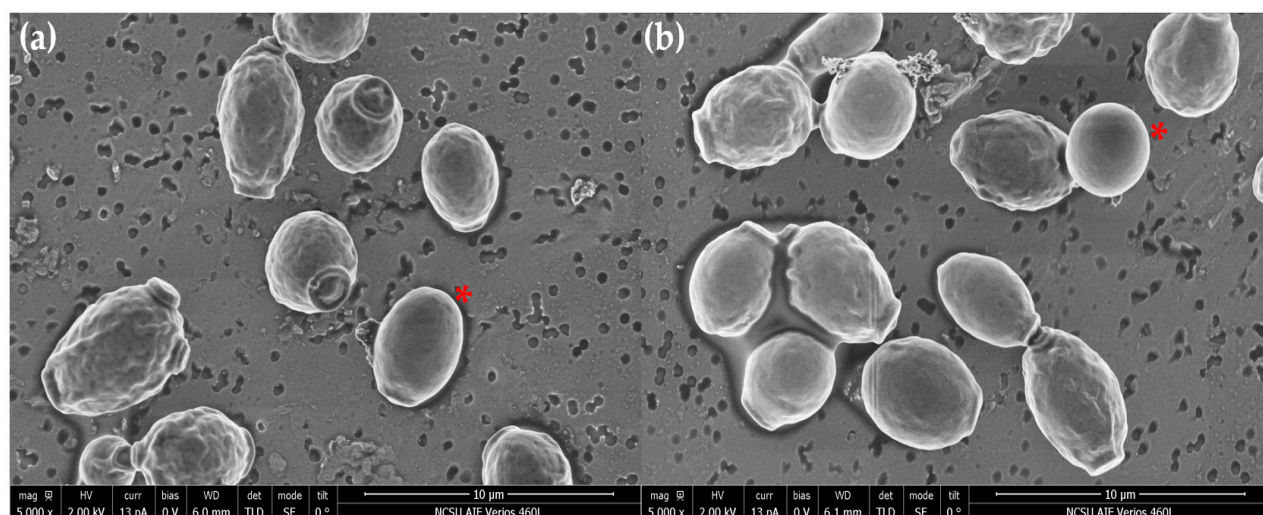


Figure 5. SEM micrographs of NS commercial (a) and NS naïve (b) yeast exposed to the MIC. The red asterisks indicate cells that do not have a drastic physical change and resemble controls.

3.4. Transmission Electron Microscopy (TEM)

TEM analysis was also used to observe the physiological responses of yeast to silver exposure. The analysis produced results for NS commercial yeast; however, results for NS

naïve yeast were inconclusive. Figure 6a shows micrographs for NS commercial yeast unexposed to AgNO_3 ; typical morphology was observed, with no visible accumulation of any particles [37,38]. The corresponding energy-dispersive X-ray spectroscopy (EDS) spectrum showed no intracellular silver accumulation (Figure 6(a1)). Abnormal morphologies were observed in NS commercial yeast exposed to the sub-MIC, with two distinct morphologies:

1. Approximately 25% of cells appeared to have mild morphological differences (cytoplasmic reduction) compared to unexposed yeast, but overall similar appearance (Figure 6c).
2. Approximately 75% of cells displayed visible disruption of the cytoplasm, enlarged vacuole, and increased periplasmic space with irregular invaginations into the cytoplasm (Figure 6b).

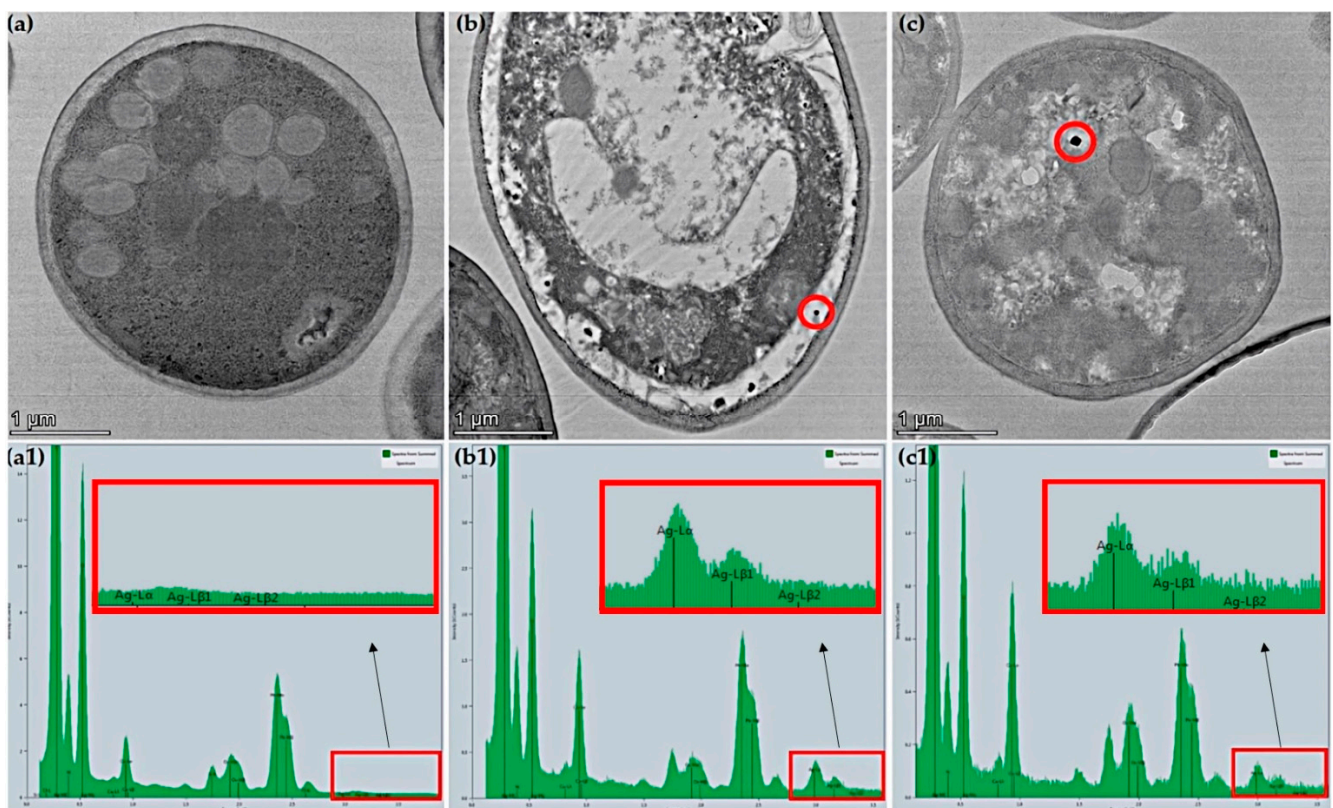


Figure 6. TEM micrographs of NS commercial yeast at 14,000 \times magnification. (a) depicts yeast exposed to 0 mg/L AgNO_3 . Both (b,c) depict yeast exposed to 22.5 mg/L AgNO_3 . The dark spots enclosed in a red circle in (b,c) are silver nanoparticles formed due to AgNO_3 exposure. (a1,b1,c1) are the EDS spectrums that correspond to the image directly above them.

NS commercial yeast exposed to the sub-MIC produced spherical/oblong silver nanoparticles that ranged from ~50 nm to ~90 nm in the widest axis end-to-end measurements (ImageJ 1.52 a). The presence of AgNPs was validated with corresponding EDS spectrums (Figure 6(b1,c1)).

3.5. ICP-OES

Due to the potential use of copper transport channels by silver ions and the potential induction of calcium signaling because of excessive metal exposure, ICP-OES was used to quantify the uptake of silver, copper, and calcium ions by *S. cerevisiae* after transient exposure to each (individually or in combination (copper and silver)). ICP-OES was also used to determine if exposure to either treatment affected the ability of cells to take up the other (silver, copper, or calcium).

Results (Figure 7) indicated that transient silver exposure resulted in a significant increase in intracellular silver concentrations in both yeast strains, which indicated the ability of yeast to internalize silver ions via some uptake mechanism. Naïve yeast had a significantly higher silver concentration (~1.7-fold) than commercial yeast, which may have been due to the smaller size (observed in SEM micrographs) of the naïve yeast, which allowed for more cells to be present in a given volume, with a greater capacity for silver uptake per volume. Silver exposure did not significantly increase copper or calcium content in either strain.

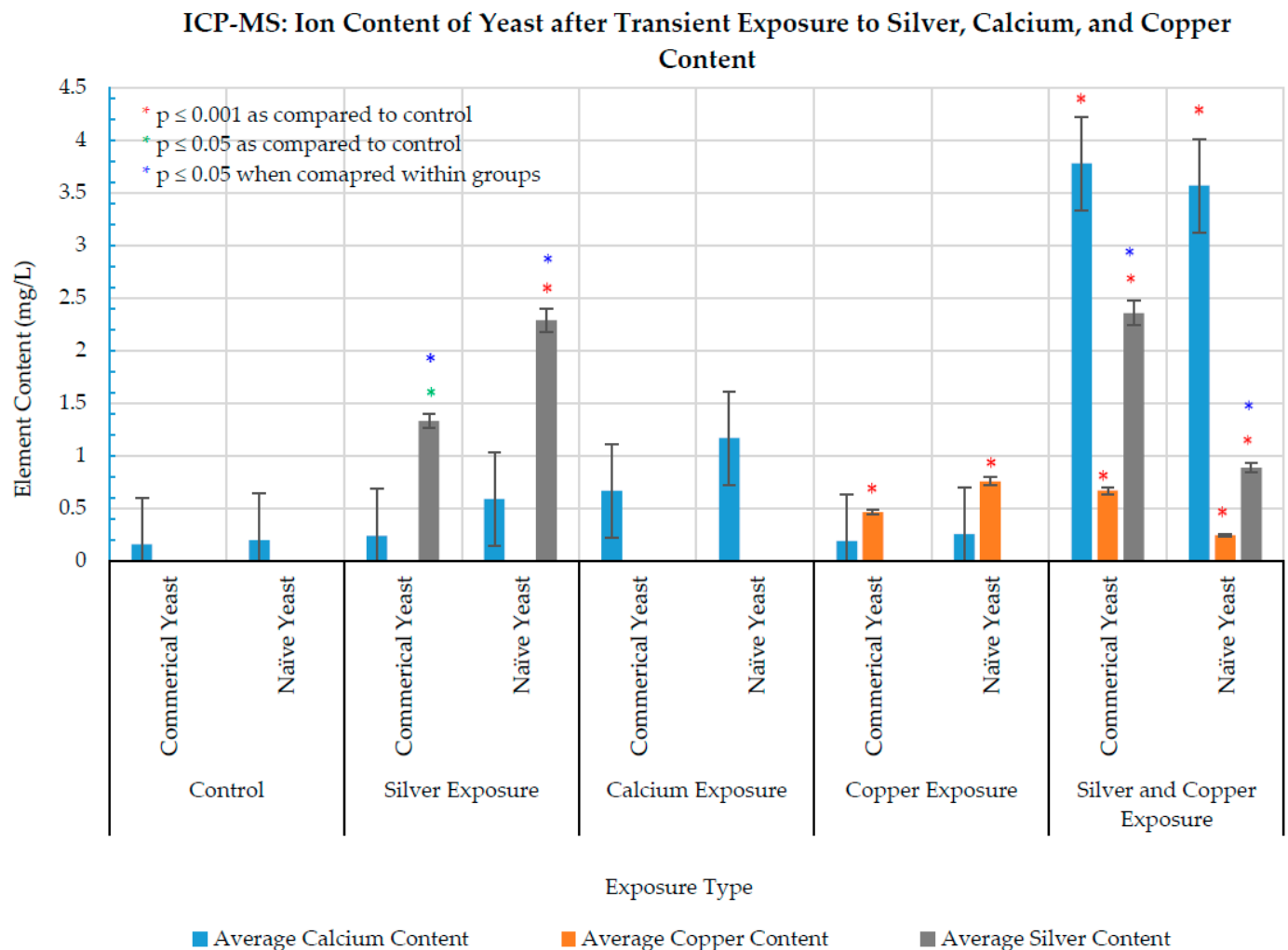


Figure 7. ICP-OES results of NS commercial ($n = 5$) and NS naïve ($n = 5$) yeast. Error bars represent percentage error (5%).

Transient copper exposure significantly increased intracellular copper concentrations in both yeast strains and did not significantly increase any other tested element. Transient calcium exposure did not significantly increase the intracellular concentrations of any tested elements. Exposure to equal concentrations of copper and silver had the most significant impact on elemental uptake, significantly increasing intracellular silver, copper, and calcium concentrations.

4. Discussion

Fungal–silver interactions are rapidly increasing; however, fungal–silver homeostasis is only partly known. In the present study, two different, nonlaboratory *S. cerevisiae* strains were studied to determine the physiological impacts of transient silver exposure and if yeast ancestral backgrounds played a role in their response to AgNO_3 .

MIC assays showed the ability of silver to inhibit all growth at 25 mg/L AgNO₃ in both strains. SEM micrographs indicated that transient silver exposure physically impaired both yeast strains by causing an indented, cratered, shrunken appearance, similar to cells exposed to silver and other toxins [22,39]. These altered-morphology indicators coincide with the reduced cell-growth results observed in MIC and growth curve assays. Silver exposure is known to downregulate genes involved in ergosterol biosynthesis (*ERG3*, *ERG5*, *ERG6*, *ERG11*, *ERG25*, and *ERG2*), which may contribute to the observed altered appearance in SEM micrographs [16,22]. This result could also be a physical representation of osmotic stress or cellular dehydration [40,41]. Similar surface alterations have also been observed in *S. cerevisiae* exposed to other stressors, signifying that this morphological change may also be a general response to stress [39]. TEM imaging showed the accumulation of silver particles due to silver exposure and abnormal intracellular appearances. Similar results exist for *S. cerevisiae* exposed to 2 mM AgNO₃ and the allergen 2S albumin [37,42]. Overall, TEM results indicated that NS commercial yeast had the capability to produce AgNPs after transient AgNO₃ exposure, even at a level of silver exposure that is detrimental to cellular growth, demonstrating *S. cerevisiae* suitability for AgNPs mycosynthesis. ICP-OES demonstrated the capacity of yeast to uptake silver. Results indicated that silver exposure only affected intracellular silver concentrations, with no significant effect on calcium or copper uptake. Coexposure to copper and silver significantly increased calcium levels. This result agrees with data that show that exposure to toxic levels of cadmium and copper (independently) resulted in a sharp increase in calcium levels [43,44]. This indicates that calcium signaling may be a response to metal stress and may play an unknown role in metal resistance and tolerance [43,44].

5. Conclusions

All results indicated that silver exposure significantly altered physiology and cell morphology, with no bias in response based on *S. cerevisiae* strain ancestral backgrounds. *S. cerevisiae* was able to withstand exposure to varying concentrations of silver, internalize and make silver nanoparticles, which may make it a useful organism for silver nanoparticle production. However, this study was not focused on using *S. cerevisiae* for AgNP production. Instead, this first report is focused on the effect of AgNO₃ on the growth physiology and morphology of *S. cerevisiae*. The current study is a prelude to further studies on the genomic and transcriptomic effects of AgNO₃ in the yeast cells studied in the experiments reported here. A full-spectrum (physiology, genomics, and transcriptomics) study about metal interactions with *S. cerevisiae* will contribute immensely to understanding metal homeostasis and cellular function in model eukaryotic cells. Such essential and in-depth knowledge is critical for the engineering and manipulation of *S. cerevisiae* for better economic importance.

Author Contributions: Conceptualization, J.R.R., O.S.I. and F.N.A.; data curation, J.R.R.; funding acquisition, O.S.I.; investigation, J.R.R. and K.S.; methodology, J.R.R. and O.S.I.; project administration, O.S.I.; resources, O.S.I.; supervision, O.S.I. and F.N.A.; writing—original draft, J.R.R.; writing—review and editing, O.S.I. and K.S. All authors have read and agreed to the published version of the manuscript.

Funding: This research was funded by a Title III HBGI Grant sponsored by the US Department of Education; Research was also supported by Evans-Allen funding through the USDA Cooperative State Research Service (USDA/Cooperative State Research, Education and Extension Service, 1400 Independence Ave., S.W. Washington, DC 20250).

Institutional Review Board Statement: Not applicable.

Informed Consent Statement: Not applicable.

Data Availability Statement: The data presented in this study are available on request from the corresponding author. The data are not publicly available due to ongoing research on this subject.

Conflicts of Interest: The authors declare no conflict of interest.

References

1. Lazić, V.; Vivod, V.; Peršin, Z.; Stoiljković, M.; Ratnayake, I.S.; Ahrenkiel, P.S.; Nedeljković, J.M.; Kokol, V. Dextran-coated silver nanoparticles for improved barrier and controlled antimicrobial properties of nanocellulose films used in food packaging. *Food Packag. Shelf Life* **2020**, *26*, 100575. [CrossRef]
2. Govindappa, M.; Lavanya, M.; Aishwarya, P.; Pai, K.; Lunked, P.; Hemashekhar, B.; Arpitha, B.; Ramachandra, Y.; Raghavendra, V.B. Synthesis and Characterization of Endophytic Fungi, *Cladosporium perangustum* Mediated Silver Nanoparticles and their Antioxidant, Anticancer and Nano-toxicological Study. *BioNanoScience* **2020**, *10*, 928–941. [CrossRef]
3. Guilger-Casagrande, M.; Lima, R.D. Synthesis of Silver Nanoparticles Mediated by Fungi: A Review. *Front. Bioeng. Biotechnol.* **2019**, *7*, 287.
4. Research, A.M. Silver Nanoparticles Market: Global Opportunity Analysis and Industry Forecast, 2020–2027. 2020, p. 509. Available online: <https://www.researchandmarkets.com/reports/5214931/silver-nanoparticles-market-by-synthesis-method> (accessed on 1 February 2022).
5. El Sayed, M.T.; El-Sayed, A.S.A. Tolerance and mycoremediation of silver ions by *Fusarium solani*. *Heliyon* **2020**, *6*, e03866. [CrossRef]
6. Priyadarshini, E.; Priyadarshini, S.S.; Cousins, B.G.; Pradhan, N. Metal-Fungus interaction: Review on cellular processes underlying heavy metal detoxification and synthesis of metal nanoparticles. *Chemosphere* **2021**, *274*, 129976. [CrossRef]
7. Ahmad, A.; Mukherjee, P.; Senapati, S.; Mandal, D.; Khan, M.I.; Kumar, R.; Sastry, M. Extracellular biosynthesis of silver nanoparticles using the fungus *Fusarium oxysporum*. *Colloids Surf. B Biointerfaces* **2003**, *28*, 313–318. [CrossRef]
8. Birla, S.S.; Gaikwad, S.C.; Gade, A.K.; Rai, M.K. Rapid Synthesis of Silver Nanoparticles from *Fusarium oxysporum* by Optimizing Physicocultural Conditions. *Sci. World J.* **2013**, *2013*, 796018. [CrossRef]
9. Du, L.; Xu, Q.; Huang, M.; Xian, L.; Feng, J.-X. Synthesis of small silver nanoparticles under light radiation by fungus *Penicillium oxalicum* and its application for the catalytic reduction of methylene blue. *Mater. Chem. Phys.* **2015**, *160*, 40–47. [CrossRef]
10. Janakiraman, V.; Govindarajan, K.; CR, M. Biosynthesis of Silver Nanoparticles from Endophytic Fungi, and its Cytotoxic Activity. *BioNanoScience* **2019**, *9*, 573–579. [CrossRef]
11. Majeed, S.; Abdullah, M.S.b.; Dash, G.K.; Ansari, M.T.; Nanda, A. Biochemical synthesis of silver nanoparticles using filamentous fungi *Penicillium decumbens* (MTCC-2494) and its efficacy against A-549 lung cancer cell line. *Chin. J. Nat. Med.* **2016**, *14*, 615–620. [CrossRef]
12. Ottoni, C.A.; Simões, M.F.; Fernandes, S.; Dos Santos, J.G.; da Silva, E.S.; de Souza, R.F.B.; Maiorano, A.E. Screening of filamentous fungi for antimicrobial silver nanoparticles synthesis. *AMB Express* **2017**, *7*, 31. [CrossRef] [PubMed]
13. Rangdist, S.; Pakdeesiriwong, N.; Chumkiew, S.; Musika, J.; Pombejra, S.N.; Nantapong, N.; Jamklang, M. Green Synthesis and Characterization of Silver Nanoparticles from Filamentous Fungi Isolated from the Environment and Their Anti-microbial Activity Against Healthcare-Associated Bacterial Pathogens. In Proceedings of the SUT International Virtual Conference on Science and Technology, Nakhon-Ratchasima, Thailand, 28 August 2020.
14. Wang, D.; Xue, B.; Wang, L.; Zhang, Y.; Liu, L.; Zhou, Y. Fungus-mediated green synthesis of nano-silver using *Aspergillus sydowii* and its antifungal/antiproliferative activities. *Sci. Rep.* **2021**, *11*, 10356. [CrossRef] [PubMed]
15. Ammar, H.A.; El Aty, A.A.A.; El AWDAN, S.A. Extracellular myco-synthesis of nano-silver using the fermentable yeasts *Pichia kudriavzevii*HA-NY2 and *Saccharomyces uvarum*HA-NY3, and their effective biomedical applications. *Bioprocess Biosyst. Eng.* **2021**, *44*, 841–854. [CrossRef] [PubMed]
16. Horstmann, C.; Campbell, C.; Kim, D.S.; Kim, K. Transcriptome profile with 20 nm silver nanoparticles in yeast. *FEMS Yeast Res.* **2019**, *19*, 1–15. [CrossRef]
17. Kudrinskiy, A.; Ivanov, A.Y.; Kulakovskaya, E.; Klimov, A.; Zherebin, P.; Khodarev, D.; Le, A.-T.; Tam, L.T.; Lisichkin, G.; Krutyakov, Y.A. The mode of action of silver and silver halides nanoparticles against *Saccharomyces cerevisiae* cells. *J. Nanopart.* **2014**, *2014*, 68635. [CrossRef]
18. Vagabov, V.; Yu Ivanov, A.; Kulakovskaya, T.; Kulakovskaya, E.; Petrov, V.; Kulaev, I. Efflux of Potassium Ions from Cells and Spheroplasts of *Saccharomyces cerevisiae* Yeast Treated with Silver and Copper Ions. *Biochemistry* **2008**, *73*, 1224–1227. [CrossRef]
19. Walker, C.; Ryu, S.; Trinh, C. Exceptional Solvent Tolerance in *Yarrowia lipolytica* Is Enhanced by Sterols. *bioRxiv* **2018**, 324681. [CrossRef]
20. Barros, D.; Pradhan, A.; Pascoal, C.; Cássio, F. Transcriptomics reveals the action mechanisms and cellular targets of citrate-coated silver nanoparticles in a ubiquitous aquatic fungus. *Environ. Pollut.* **2021**, *268*, 115913. [CrossRef]
21. Das, D.; Ahmed, G. Silver nanoparticles damage yeast cell wall. *J. Biotechnol.* **2012**, *3*, 36–39.
22. Radhakrishnan, V.S.; Reddy Mudiam, M.K.; Kumar, M.; Dwivedi, S.P.; Singh, S.P.; Prasad, T. Silver nanoparticles induced alterations in multiple cellular targets, which are critical for drug susceptibilities and pathogenicity in fungal pathogen (*Candida albicans*). *Int. J. Nanomed.* **2018**, *13*, 2647–2663. [CrossRef]
23. Szerencsés, B.; Igaz, N.; Tóbiás, Á.; Prucsi, Z.; Rónavári, A.; Béteky, P.; Madarász, D.; Papp, C.; Makra, I.; Vágvölgyi, C.; et al. Size-dependent activity of silver nanoparticles on the morphological switch and biofilm formation of opportunistic pathogenic yeasts. *BMC Microbiol.* **2020**, *20*, 176. [CrossRef] [PubMed]
24. Robinson, J.R.; Isikhuemhen, O.S.; Anike, F.N. Fungal–Metal Interactions: A Review of Toxicity and Homeostasis. *J. Fungi* **2021**, *7*, 225. [CrossRef] [PubMed]

25. White, T.J.; Bruns, T.; Lee, S.; Taylor, J. Amplification and direct sequencing of fungal ribosomal RNA genes for phylogenetics. *PCR Protoc. Guide Methods Appl.* **1990**, *18*, 315–322.
26. Gold, M.; Cheng, T. Induction of colonial growth and replica plating of the white rot basidiomycete *Phanaerochaete chrysosporium*. *Appl. Env. Microbiol.* **1978**, *35*, 1223–1225. [\[CrossRef\]](#)
27. Shifrine, M.; Phaff, H.; Demain, A. Determination of carbon assimilation patterns of yeasts by replica plating. *J. Bacteriol.* **1954**, *68*, 28–35. [\[CrossRef\]](#)
28. Despax, B.; Saulou, C.; Raynaud, P.; Datas, L.; Mercier-Bonin, M. Transmission electron microscopy for elucidating the impact of silver-based treatments (ionic silver versus nanosilver-containing coating) on the model yeast *Saccharomyces cerevisiae*. *J. Nanotechnol.* **2011**, *22*, 175101. [\[CrossRef\]](#)
29. Klaus, T.; Joerger, R.; Olsson, E.; Granqvist, C.-G. Silver-based crystalline nanoparticles, microbially fabricated. *Proc. Natl. Acad. Sci. USA* **1999**, *96*, 13611–13614. [\[CrossRef\]](#)
30. Saulou, C.; Jamme, F.; Maranges, C.; Fourquaux, I.; Despax, B.; Raynaud, P.; Dumas, P.; Mercier-Bonin, M. Synchrotron FTIR microspectroscopy of the yeast *Saccharomyces cerevisiae* after exposure to plasma-deposited nanosilver-containing coating. *Anal. Bioanal. Chem.* **2010**, *396*, 1441–1450. [\[CrossRef\]](#)
31. Vazquez-Muñoz, R.; Avalos-Borja, M.; Castro-Longoria, E. Ultrastructural analysis of *Candida albicans* when exposed to silver nanoparticles. *PLoS ONE* **2014**, *9*, e108876. [\[CrossRef\]](#)
32. Alsuhaim, H.; Vojisavljevic, V.; Pirogova, E. Effects of non-thermal microwave exposures on the proliferation rate of *saccharomyces cerevisiae* yeast. In *World Congress on Medical Physics and Biomedical Engineering*; Springer: Berlin/Heidelberg, Germany, 2012.
33. Do, A.; Sakai, T.; Kishida, M.; Furuta, M. Isolation and Characterization of a Variant Manganese Resistant Strain of *Saccharomyces cerevisiae*. *Biocontrol. Sci.* **2016**, *21*, 253–260. [\[CrossRef\]](#)
34. Du, Y.; Cheng, W.; Li, W.-F. Expression Profiling Reveals an Unexpected Growth-Stimulating Effect of Surplus Iron on the Yeast *Saccharomyces cerevisiae*. *Mol. Cells* **2012**, *34*, 127–132. [\[CrossRef\]](#) [\[PubMed\]](#)
35. Geva, P.; Kahta, R.; Nakonechny, F.; Aronov, S.; Nisnevitch, M. Increased copper bioremediation ability of new transgenic and adapted *Saccharomyces cerevisiae* strains. *Environ. Sci. Pollut. Res.* **2016**, *23*. [\[CrossRef\]](#) [\[PubMed\]](#)
36. Luo, F.; Zhu, S.; Hu, Y.; Yang, K.-C.; He, M.-S.; Zhu, B.; Wang, G.-X.; Ling, F. Biocompatibility assessment of Fe₃O₄ nanoparticles using *Saccharomyces cerevisiae* as a model organism. *Comp. Biochem. Physiol. Part C Toxicol. Pharmacol.* **2020**, *227*, 108645. [\[CrossRef\]](#) [\[PubMed\]](#)
37. Agizzio, A.; Cunha, M.; de Oliveira Carvalho, A.; de Oliveira, M.A.; Ribeiro, S.; Gomes, V. The antifungal properties of a 2S albumin-homologous protein from passion fruit seeds involve plasma membrane permeabilization and ultrastructural alterations in yeast cells. *Plant Sci.* **2006**, *171*, 523–530. [\[CrossRef\]](#)
38. Moreira, L.M.C.; Ribeiro, F.H.; Neves, M.J.; Porto, B.A.A.; Amaral, A.M.; Menezes, M.A.B.; Rosa, C.A. Response of *Saccharomyces cerevisiae* to cadmium stress. In Proceedings of the 2009 International Nuclear Atlantic Conference-INAC 2009, Rio de Janeiro, Brazil, 27 September–2 October 2009; Available online: https://inis.iaea.org/search/search.aspx?orig_q=RN:40103886 (accessed on 1 February 2022).
39. Bennis, S.; Chami, F.; Chami, N.; Bouchikhi, T.; Remmal, A. Surface alteration of *Saccharomyces cerevisiae* induced by thymol and eugenol. *Lett. Appl. Microbiol.* **2004**, *38*, 454–458. [\[CrossRef\]](#)
40. Borovikova, D.; Teparić, R.; Mrša, V.; Rapoport, A. Anhydrobiosis in yeast: Cell wall mannoproteins are important for yeast *Saccharomyces cerevisiae* resistance to dehydration. *Yeast* **2016**, *33*, 347–353. [\[CrossRef\]](#)
41. Saldaña, C.; Villava, C.; Ramírez-Villarreal, J.; Morales-Tlalpan, V.; Campos-Guillen, J.; Chávez-Servín, J.; García-Gasca, T. Rapid and reversible cell volume changes in response to osmotic stress in yeast. *Braz. J. Microbiol.* **2021**, *52*, 895–903. [\[CrossRef\]](#)
42. Ruta, L.; Popa, C.V.; Nicolau, I.; Farcasanu, I. Calcium signaling and copper toxicity in *Saccharomyces cerevisiae* cells. *Environ. Sci. Pollut. Res.* **2016**, *23*. [\[CrossRef\]](#)
43. Ruta, L.L.; Popa, V.C.; Nicolau, I.; Danet, A.F.; Iordache, V.; Neagoe, A.D.; Farcasanu, I.C. Calcium signaling mediates the response to cadmium toxicity in *Saccharomyces cerevisiae* cells. *FEBS Lett.* **2014**, *588*, 3202–3212. [\[CrossRef\]](#)
44. Lekha, D.C.; Shanmugam, R.; Madhuri, K.; Dwarampudi, L.P.; Bhaskaran, M.; Kongara, D.; Tesfaye, J.L.; Nagaprasad, N.; Bhargavi, V.L.N.; Krishnaraj, R. Review on Silver Nanoparticle Synthesis Method, Antibacterial Activity, Drug Delivery Vehicles, and Toxicity Pathways: Recent Advances and Future Aspects. *J. Nanomater.* **2021**, *2021*, 4401829. [\[CrossRef\]](#)